Development 128, 1547-1558 (2001)
Printed in Great Britain © The Company of Biologists Limited 2001
DEV2690

Overexpression of *Hoxc13* in differentiating keratinocytes results in downregulation of a novel hair keratin gene cluster and alopecia

Andrei V. Tkatchenko[1,*], Richard P. Visconti[2], Lijuan Shang[1], Thomas Papenbrock[1,‡], Nathanael D. Pruett[1], Tatsuya Ito[1], Makio Ogawa[1,3] and Alexander Awgulewitsch[1,3,§]

[1]Department of Medicine, Medical University of South Carolina, Charleston, SC 29425, USA
[2]Department of Cell Biology and Anatomy, Medical University of South Carolina, Charleston, SC 29425, USA
[3]Hollings Cancer Center, Medical University of South Carolina, Charleston, SC 29425, USA
*Present address: Department of Neurobiology, Harvard Medical School, Boston, MA 02115, USA
‡Present address: School of Biological Sciences, University of Southampton, Southampton SO16 7PX, UK
§Author for correspondence (e-mail: awgulewa@musc.edu)

Accepted 16 February; published on WWW 5 April 2001

SUMMARY

Studying the roles of Hox genes in normal and pathological development of skin and hair requires identification of downstream target genes in genetically defined animal models. We show that transgenic mice overexpressing *Hoxc13* in differentiating keratinocytes of hair follicles develop alopecia, accompanied by a progressive pathological skin condition that resembles ichthyosis. Large-scale analysis of differential gene expression in postnatal skin of these mice identified 16 previously unknown and 13 known genes as presumptive Hoxc13 targets. The majority of these targets are downregulated and belong to a subgroup of genes that encode hair-specific keratin-associated proteins (KAPs). Genomic mapping using a mouse hamster radiation hybrid panel showed these genes to reside in a novel KAP gene cluster on mouse chromosome 16 in a region of conserved linkage with human chromosome 21q22.11. Furthermore, data obtained by *Hoxc13/lacZ* reporter gene analysis in mice that overexpress *Hoxc13* suggest negative autoregulatory feedback control of *Hoxc13* expression levels, thus providing an entry point for elucidating currently unknown mechanisms that are required for regulating quantitative levels of Hox gene expression. Combined, these results provide a framework for understanding molecular mechanisms of *Hoxc13* function in hair growth and development.

Key words: Hoxc13, Transgenic, Target genes, Alopecia, KAP gene cluster, Mouse

INTRODUCTION

Development of skin and hair evidently employs many of the regulatory mechanisms used elsewhere during organogenesis (Oro and Scott, 1998). Based on their distinct spatio-temporal expression patterns in both developing and adult skin, many members of the phylogenetically conserved Hox gene family have been implicated in the patterning, growth and cyclical regenerative processes of skin and hair, as well as in certain skin pathologies including cancer (e.g. Scott and Goldsmith, 1993; Stelnicki et al., 1998; Chang et al., 1998). Although many of the embryonic patterning functions of Hox genes have been successfully defined by gene targeting (reviewed by Krumlauf, 1994; Capecchi, 1997), Hox mutant mice frequently suffer from perinatal lethality, thus precluding analysis of their presumptive roles in postnatal skin and hair follicles. Accordingly, the hairlessness observed in *Hoxc13* loss-of-function mutants is to date the only reported case of a Hox mutant with a skin phenotype (Godwin and Capecchi, 1998). Although these mice develop morphologically normal hair follicles, the brittleness of the rudimentary hair produced causes it to break off at the surface. In interpreting these results, it has been proposed that *Hoxc13* may either directly or indirectly regulate hair-specific keratin genes or, alternatively, play a role in controlling proliferation and differentiation of follicular keratinocytes involved in hair growth.

Hox genes encode transcription factors that have been postulated to act as master switches in development by controlling the activities of batteries of downstream 'realisator' genes, also referred to as cytodifferentiation or structural genes (Garcia-Bellido, 1975; Gehring, 1987). Consequently, defining the roles of Hox genes at molecular levels will require identification of these downstream targets in animal models that harbor defined genetic alterations. Information about Hox targets, however, is presently rather tenuous and most of the relatively small number of target genes have been identified in the fruit fly *Drosophila* (reviewed by Graba et al., 1997). In keeping with the diversity of cell types and developmental stages where Hox genes are expressed, these target genes exhibit great heterogeneity and may be grouped into three major functional classes, including regulatory genes that encode either transcription factors or signaling molecules, and the realisator genes, whose products are believed to be directly involved in terminal differentiation. To date, the isolation of

clusters of structurally and functionally similar Hox target genes that might correspond to the hypothesized realisator gene batteries has been elusive.

Studies with both Hox gain- and loss-of-function mutants suggest that the patterning functions of Hox genes are sensitive to their quantitative levels of expression (Pollock et al., 1992; Capecchi, 1997; Greer et al., 2000). This implies existence of control mechanisms that keep the concentration of specific Hox gene products within the range of critical threshold levels. It has been proposed that negative autoregulatory feedback might be a fundamental mechanism for providing this type of stability in expression of transcriptional regulators (Savageau, 1974; Thieffry et al., 1998). While recent data obtained with synthetic gene networks engineered in *Escherichia coli* support this concept (Becskei and Serrano, 2000), its in vivo validity in eucaryotic systems has not yet been demonstrated.

We have addressed essential aspects of these issues by using a transgenic mouse model overexpressing *Hoxc13*, termed GC13 mice. Our data show that overexpression of *Hoxc13* in differentiating keratinocytes of hair follicles results in alopecia. We provide evidence for the existence of a negative autoregulatory feedback loop controlling *Hoxc13* expression levels in hair follicles by examining expression of a *Hoxc13-lacZ* reporter gene construct in both normal and GC13 mutants. By using suppression subtractive hybridization (Diatchenko et al., 1996) of cDNAs derived from normal versus GC13 postnatal skin, we have isolated differentially expressed genes as downstream targets of Hoxc13. Consistent with the hair defect, we found that among these genes the largest group consisted of novel, as well as previously known, keratin-associated protein (KAP)-encoding genes, whose expression was repressed by up to more than 20-fold in GC13 skin. Using a mouse-hamster radiation hybrid gene panel, we mapped most of these genes to a narrow distal region of mouse chromosome 16 syntenic to human chromosome 21, thus revealing the existence of a novel KAP gene cluster.

MATERIALS AND METHODS

Sequence analysis

The *Hoxc13*-coding sequence was derived from overlapping cDNAs obtained by 5′ and 3′ RACE (rapid amplification of cDNA ends) and confirmed by analysis of corresponding genomic sequences. Total RNA isolated from the posterior halves of E12 embryos was used as template for cDNA synthesis. The presumptive start codon is the most distal ATG of a continuous open reading frame positioned in a sequence context that resembles a common consensus for eucaryotic translational initiation (Kozak, 1983). Differentially expressed cDNA sequences were analyzed by searching public databases for sequence similarities using Advanced Blast program at NCBI.

Generation of transgenes and transgenic mice

The GC13 overexpression construct was derived from cosmid cos2W3H (Peterson et al., 1994) as a 19 kb *Not*I-*Xho*I fragment and subcloned. Reporter gene construct LZ-GC13 was generated by replacing a singular *Asc*I fragment of GC13 that contained 430 bp of the 3′-region of *Hoxc13* exon 1 and approximately 50 bp of adjacent intronic sequences (Fig. 1A) with PCR-amplified *E. coli lacZ*, thus creating an in-frame-fusion between the *Hoxc13*- and *lacZ*-coding sequences. The *lacZ* gene was amplified from plasmid pCH110 (Amersham Pharmacia) and *Asc*I restriction sites were incorporated by PCR using, respectively, the following forward and reverse primers: 5′-GGCGCGCCAAGTCGTTTTACAACGTCGTGACTGG-3′; 5′-GGCGCGCCCTTACGCGAAATACGGGCAGAC-3′. GC13 transgenic mice were generated by pronuclear injection of FVB zygotes and mutant 61B1 and 61U4 transgenic lines were established by breeding with FVB mice. In both lines the mutant trait was transmitted to subsequent generations without recognizable changes. Transgenesis was determined by PCR analysis of genomic DNA isolated from tail biopsies or placentas. Forward and reverse primers 5′GGAGAGCCTGGGCGTAGACATC and 5′CCAATTTGCCTCC-CTTTTCTGGTCC derived from sequences near the 3′ and 5′ ends of GC13, respectively, amplified a diagnostic 400 bp fragment that assumed tandem incorporation of multiple transgene copies. Injection of embryos with LZ-GC13 resulted in a total of six transgenic mice expressing *lacZ* in the same pattern (see Fig. 3) as examined by X-gal staining, essentially as described (Papenbrock et al., 1998). Three of these mice were sacrificed and examined at different embryonic stages, while the remaining were used as founders for establishing three independent LZ-GC13 strains used for further analyses. Preliminary blood and bone marrow analysis of GC13 mutant mice did not reveal hematopoietic defects as a potential cause for the frequent perinatal lethality (data not shown).

In situ hybridization

Whole-mount in situ hybridization in E13-E15 embryos was performed as described (Hogan et al., 1994) by using digoxigenin-labeled (Roche Diagnostics) antisense RNA probes synthesized either from plasmid pc13ISH (Peterson et al., 1994), or from plasmid pC13rev containing a partial cDNA of 697 bp that included 532 bp of 3′ coding sequence and 165 bp of 3′ untranslated flanking sequence cloned into vector pCRII-TOPO (Invitrogen). Between the two probes, no difference in expression pattern and signal intensity was detectable. In situ hybridization to 10 μm frozen skin sections using ^{35}S-labeled sense and antisense (control) RNA probes synthesized from pC13rev was performed at 50°C as described (Awgulewitsch and Utset, 1991). Samples were exposed to Kodak NTB2 autoradiographic photoemulsion for 4 days.

BrdU assays and immunofluorescence microscopy

Pieces of skin (approx. 0.3×1.0 cm) dissected from anterior dorsal trunk of 2-day-old postnatal mice were incubated in RPMI medium supplemented with 100 μM BrdU for 4 hours, fixed in 3% paraformaldehyde for 30 minutes, and embedded in Tissue-Tek™ OCT compound (Sakura Finetechnical, Tokyo). Cryosections (10 μm) were stained with rabbit anti-β-galactosidase (β-gal) polyclonal antibodies (Eppendorf – 5 Prime), followed by rhodamine-conjugated donkey anti-rabbit IgG (Chemicon International). For BrdU/β-gal double-staining, sections were additionally incubated with FastImmune Anti-BrdU FITC-conjugated antibodies with DNase (Becton Dickinson Immunocytometry Systems) for 45 minutes at room temperature and fixed in 1% paraformaldehyde for 5 minutes before mounting in ProLong™ Antifade Reagent (Molecular Probes). Image analysis was performed using a Leitz™ photomicroscope equipped with a Photometrics™ Quantix CCD camera.

Differential screening

Screening for differentially expressed genes in skin of GC13 mice was performed essentially as described previously (Tkatchenko et al., 2000). Subtracted/normalized cDNA libraries were generated using the PCR-Select cDNA Subtraction Kit (Clontech). Secondary PCR products were cloned into pCRII-TOPO vector using TOPO TA Cloning Kit (Invitrogen) and resulting libraries were organized in 384-well plates. Bacterial clones from these plates were manually printed onto Hybond-XL nylon membranes (Amersham Pharmacia Biotech) using a 384 pin tool (V&P Scientific) to prepare two identical sets of bacterial colony filters. Hybridization of duplicate filters containing 384 randomly picked clones of either library with subtracted cDNA probes detected 130 differential signals corresponding to 71 under-

and 59 overexpressed sequences. Sequence analysis of these cDNAs identified a total of 74 different known and unknown sequences, thus revealing an average redundancy of 1.8. High density array filters were prepared with these potentially differential cDNAs to determine their relative levels of expression in normal and GC13 mutant skin by reverse Northern quantitative hybridization as described (Tkatchenko et al., 2000).

Phylogenetic tree analysis and genomic mapping

Phylogenetic tree analysis of amino acid sequences deduced from KAP-related cDNA sequences was performed by using the Genebee Multiple Alignment program (Belozersky Institute, Moscow State University; http://www.genebee.msu.su/services/malign_reduced.html). For GenBank Accession Numbers of previously known and novel KAP gene sequences used for this analysis, see Fig. 6A.

Known and novel KAP genes were mapped by using a mouse/hamster radiation hybrid (RH) panel (Research Genetics). PCR data sets obtained with this panel were analysed at the Jackson Laboratory RH database (http://www.jax.org/resources/documents/cmdata) for determining genomic map positions. PCR cycling conditions were 95°C for 7 minutes; 32 cycles of 94°C for 30 seconds; Ta (optimized annealing temperature) for 35 seconds; 72°C for 45 seconds; 72°C for 5 minutes. Under these conditions, Ta and pair of forward (F) and reverse (R) primers used for each gene analyzed were as follows:

HGTpII.1 (62°C), F/5′GGCTGTGGTTATGGCTCCTA; R/5′GTGAAGAATGGCAAAGTCCTG;

Pmg1 (62°C), F/5′GATGTGGTACCCCTACTTTCT; R/5′GTTTTGCCAATTACAGGAACTC;

Hacl1 (70°C), F/5′GCCCAGTTACCACAGCCTCAG; R/5′GGCGTAGAGCAAGGATTGGAG;

krtap16-1 (56°C), F/5′TGGAGGATATGGGTTCTC; R/5′CATGTTCAGTTGGCTTAGTAC;

krtap16-2 (56°C), F/5′GGACTTGGAAATACTTGTCG; R/5′TGGGAATGTGTTGTAGAGG;

krtap16-3 (60°C), F/5′GTGGAGGATATGGGTTCTC; R/5′CTGCAACAATGTTATTGACTG;

krtap16-4 (56°C), F/5′CTATGGCTCTGGAGGCTATG; R/5′GAGTTGCTTTCCCAGTTCAG;

krtap16-5 (56°C), F/5′AATCCTGTTCCAGTAACTCAG; R/5′ACATAATCCCACTCTTAGTGC;

krtap16-6 (58°C), F/5′GTGGAGGATATGGGTTCTC; R/5′CTGCAACAATGTTATTGACTG;

krtap16-7 (60°C), F/5′TGTGCTGCAACTACTACGG; R/5′GCCATATCCACAGCCATAT; and

krtap16-8 (56°C), F/5′CTATGGCTGTGGCTACCG; R/5′ACATGCAGTTCAGAATTGGAG.

Scanning electron microscopy

Samples were attached onto specimen stubs using double-stick conductive tabs and sputter-coated with gold using a Polaron SEM Coating Unit # 5150. Samples were imaged using a JEOL JSM 5410 LV Scanning Electron Microscope.

RESULTS

GC13 transgenic mice exhibit severe hair and skin defects

To further assess the role of *Hoxc13* in hair growth, we generated transgenic mice that overexpressed this gene,

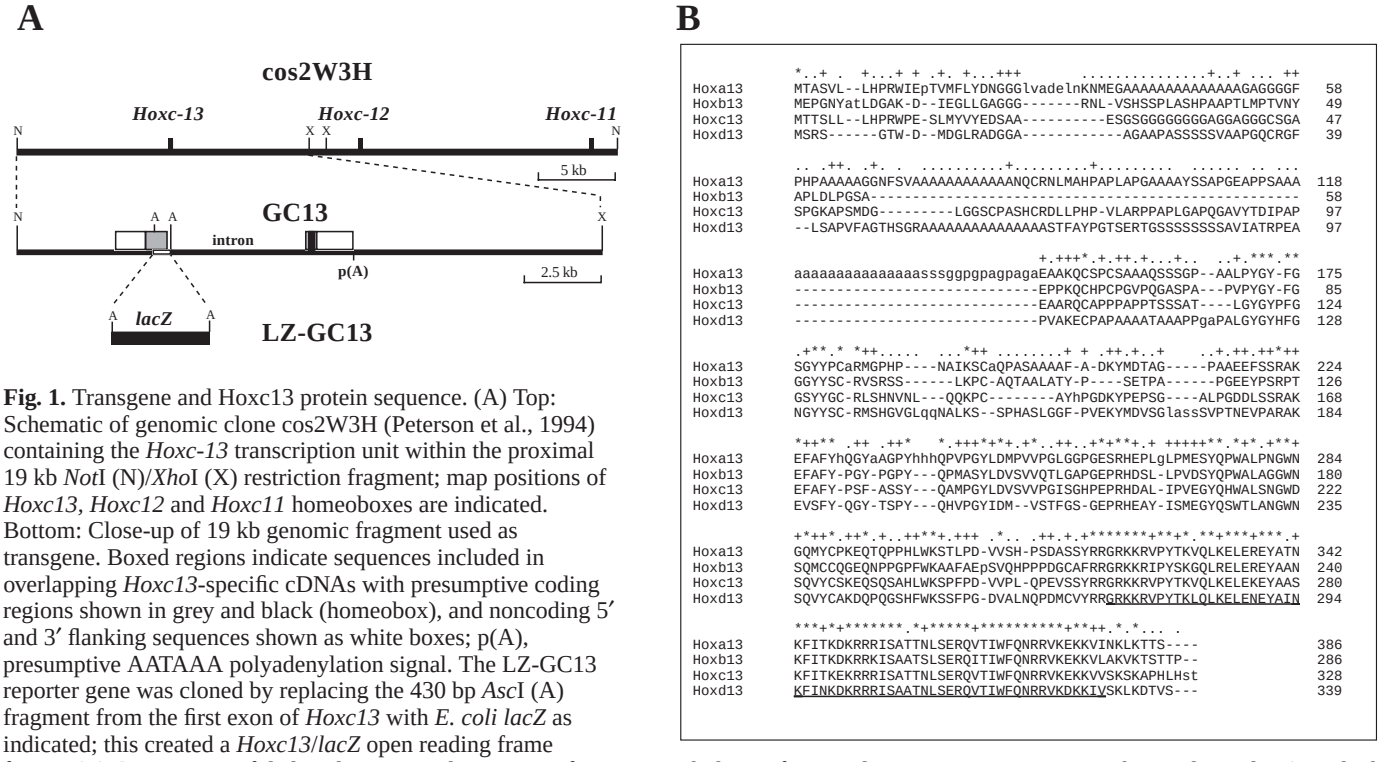

Fig. 1. Transgene and Hoxc13 protein sequence. (A) Top: Schematic of genomic clone cos2W3H (Peterson et al., 1994) containing the *Hoxc-13* transcription unit within the proximal 19 kb *Not*I (N)/*Xho*I (X) restriction fragment; map positions of *Hoxc13*, *Hoxc12* and *Hoxc11* homeoboxes are indicated. Bottom: Close-up of 19 kb genomic fragment used as transgene. Boxed regions indicate sequences included in overlapping *Hoxc13*-specific cDNAs with presumptive coding regions shown in grey and black (homeobox), and noncoding 5′ and 3′ flanking sequences shown as white boxes; p(A), presumptive AATAAA polyadenylation signal. The LZ-GC13 reporter gene was cloned by replacing the 430 bp *Asc*I (A) fragment from the first exon of *Hoxc13* with *E. coli lacZ* as indicated; this created a *Hoxc13*/*lacZ* open reading frame fusion. (B) Comparison of deduced amino acid sequence of *Hoxc13* with those of its paralogous genes *Hoxa13*, *Hoxb13* and *Hoxd13* (Mortlock et al., 1996; Zeltser et al., 1996; Hérault et al., 1996). Signs shown at top of the alignment indicate the following degrees of sequence conservation: no sign, average weight of column pair exchanges is less than weight matrix mean value; black dot, average weight of column pair exchanges is less than mean value plus one s.d.; + , average weight of column pair exchanges is less than mean value plus two s.d.; *, average weight of column pair exchanges is more than mean value plus two s.d. The homoedomain is underlined. The *Hoxc13*-coding sequence has been deposited in the GenBank database, Accession Number AF193796.

employing as a transgene a 19 kb genomic fragment (GC13) containing *Hoxc13* (Fig. 1A). Based on genomic and cDNA sequencing, we determined the deduced protein sequence of 328 amino acid residues containing the Hoxc13 homeodomain (Peterson et al., 1994) near its C terminus (Fig. 1B). Sequence comparison revealed, outside the homeodomain, partial similarity at the N terminus to the other three paralogous group 13 Hox proteins (Mortlock et al., 1996; Zeltser et al., 1996; Hérault et al., 1996).

We established two GC13 mutant transgenic lines (61B1 and 61U4) of essentially identical phenotype (Fig. 2). Mutant mice could be identified at birth by a short tail and taut skin (Fig. 2A, part a), as well as kinky whiskers (Fig. 2A, part c), and frequently an overall smaller stature in comparison to non-transgenic littermates (Fig. 2A, part a). Juvenile mutants exhibited retarded growth of coat hair (Fig. 2A, part a), while adult animals developed progressive alopecia and flakiness of the skin at varying degrees (Fig. 2A, part b). Regions most severely affected were ventral and anterior-dorsal trunk and head. Skeletal analysis revealed that the shorter tail was due to a reduction in the number of tail vertebrae by about ten (Fig. 2A, parts e,f). This loss affected exclusively caudal vertebrae without lateral processes and did not involve homeotic transformations of any of the five most anterior caudal vertebrae C1 through C5, which continued to have lateral processes (Fig. 2A, parts e,f).

The overtly recognizable and, with age, rapidly advancing pathological changes in mutant skin were mirrored by progressive histological abnormalities (Fig. 2B). Most obvious changes were epidermal thickening and enlarged hair follicles; the former was apparent already in 5-day-old postnatal skin (Fig. 2B), which is when hair follicles are in the growth phase (anagen) of the first hair cycle (Paus et al., 1999). Follicle enlargement appeared to result primarily from thickened outer root sheaths (ORSs), as observed in anagen follicles of the second hair cycle in 30-day-old skin. In skin of adult mutants older than 2-3 months, many follicles had degenerated into cyst-like structures filled with large amounts of (presumably) keratinaceous material (Fig. 2B). Both the squamous and suprabasal cellular layers, which appeared overall irregular and disorganized, contributed to the dramatic epidermal thickening, underlying the scaly appearance of the skin characteristic of ichthyosis. Severely affected animals typically exhibited ulceration of the skin (data not shown). Scanning electron microscopy of mutant whisker shafts

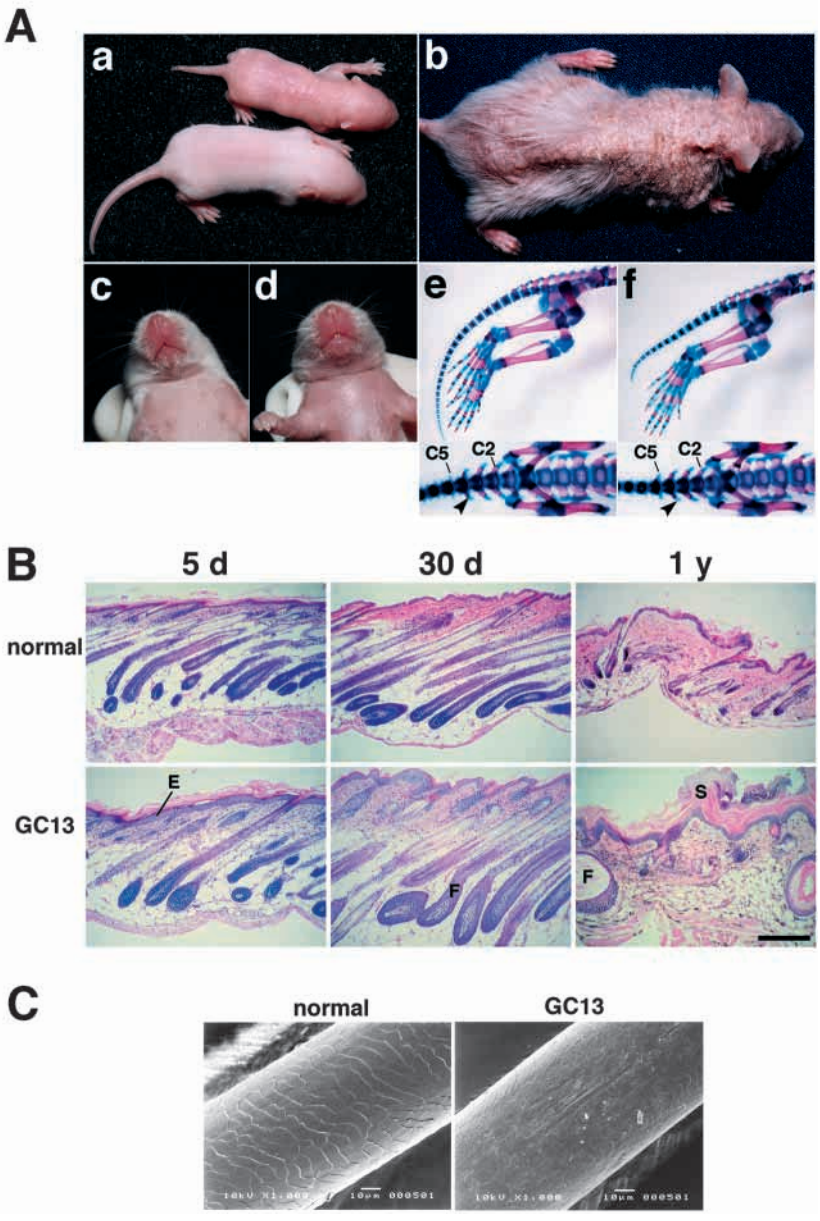

Fig. 2. Phenotypic changes in transgenic mice overexpressing *Hoxc13*. (A) Externally discernible changes of skin and skeleton. (a) One week old GC13 (61B1) mutant pup (top) in comparison with non-transgenic littermate (below); note the smaller size, shorter tail and retardation of hair growth exhibited by the mutant. (b) dorsal view of 4.5-month-old GC13 (61U4) mutant female mouse exhibiting severe scaling and crusting of skin, as well as alopecia. Ventral/facial view of a 10-day-old GC13 (61B1) mutant pup (d) in comparison with non-transgenic littermate (c) shows retarded growth of ventral hair coat and kinkiness of mutant whiskers. Alcian Blue and Alizarin Red staining of posterior skeletons of 2-day-old (61B1) mutant (f) and non-transgenic littermate (e) reveals reduction in the number of tail vertebrae in the mutant; ventral view of sacral and caudal vertebrae C1 through C5 shows no changes in the number of vertebrae with lateral processes (arrowheads) between mutant and control. (B) Hematoxylin and Eosin stained sagittal sections (5 μm) of dorsal neck skin derived from normal and GC13 mutant (61B1) littermates sacrificed at 5 days, 30 days and 1 year of age; note the thickened cellular epidermis (E) in mutant skin of each stage and the enormously thickened squamous layer (S) in older mutants; enlargement of mutant anagen hair follicles (F) seen at 30 days appears to result from thickened outer root sheaths; older GC13 mice have distended, cyst-like follicles. (C) Scanning electron micrographs of nasal whiskers from 3-month-old normal and GC13 (61B1) mutant mice. Scale bar in B: 200 μm for B.

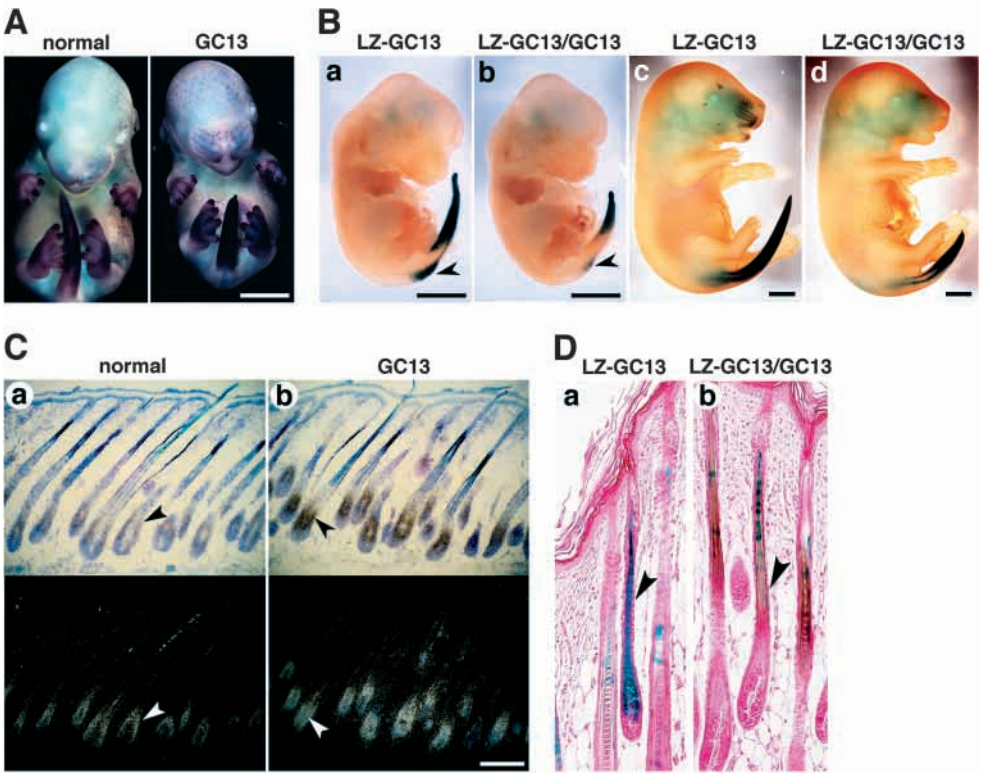

Fig. 3. Analysis of *Hoxc13* and LZ-GC13 reporter gene expression patterns. (A) Detection of *Hoxc13* expression pattern in tail, limbs and skin of E15 normal and GC13 mutant embryos by whole-mount in situ hybridization (WMISH) with *Hoxc13*-specific RNA probe reveals increased hybridization signal (purple) in tail bud and vibrissae, as well as in developing coat hair follicles of mutant (right) versus normal (left) embryo. (B) X-gal staining (dark blue) of normal LZ-GC13 (a,c) and mutant LZ-GC13/GC13 (b,d) transgenic embryos at E13 (a,b) and E16.5 (c,d); note reduced X-gal staining in neural tube (arrowhead) and tail bud of E13 double transgenic mutant (b), and in tail bud, vibrissae and pelage hair follicles of E16.5 mutant (d) compared with normal embryos (a,c). (C) In situ hybridization in 10 μm sections of 5-day-old normal (a) and GC13 mutant (b) skin using ^{35}S-labeled *Hoxc13*-specific antisense probe; note increased hybridization signals over upper bulb and lower shaft regions (arrowheads) of mutant (b) versus normal (a) hair follicles viewed in bright- (top) and darkfield (bottom), whereas no specific hybridization signal is detectable over epidermal cells. (D) X-gal staining (blue) in Eosin counterstained 5 μm sections of 5-day-old dorsal neck skin of normal LZ-GC13 (a) and mutant LZ-GC13/GC13 (b) pup; note strongest staining in normal hair follicle (arrowhead) extending from upper regions of the bulb to the hairshaft (a), regions known to contain differentiating keratinocytes (Fuchs et al., 1995), whereas a mutant follicle of approximately the same stage (arrowhead in b) exhibits reduced X-gal staining (blue and brownish color) in mid-regions of the shaft and no staining in the upper bulb region. Scale bars: 2 mm in A,B; 200 μm in C.

revealed changes in cuticular septation that often exhibited lesions and appeared generally denser and less well defined (Fig. 2C). These architectural defects were mirrored by lack of or irregular septation in plucked mutant coat hair, which often showed fracturing near the root (data not shown).

Negative autoregulatory feedback control of Hoxc13 expression

Mutant embryos at stages E13 through E15 exhibited higher levels of *Hoxc13* expression exclusively in those structures that we observed to be phenotypically affected, namely vibrissae and tail bud at E13 (data not shown), as well as pelage hair follicles beginning at E15 (Fig. 3A). These data suggest the presence of control elements required for *Hoxc13* expression in developing hair follicles and tail bud within the GC13 transgene. This assumption was confirmed by analyzing the expression pattern of a *lacZ*-tagged version of the GC13 transgene termed LZ-GC13 (Fig. 1A), which was expressed in tailbud and vibrissae at E13, and in coat hair follicles at later (≥E15) stages (Fig. 3B, parts a,c). To monitor LZ-GC13 expression in GC13 mutant background, we generated LZ-GC13/GC13 double transgenic mice. Surprisingly, these mutant mice showed reduced levels of X-gal staining in neural tube and tail at E13 (compare Fig. 3B, part a with Fig. 3B, part b), as well as in vibrissae and developing pelage hair follicles at E16.5 (Fig. 3B, parts c,d), i.e. the same sites where we detected increased levels of *Hoxc13* expression by WMISH in GC13 mice (Fig. 3A). These results suggest the existence of a negative autoregulatory feedback loop, which is probably required for maintaining balanced physiological levels of *Hoxc13* expression. To obtain evidence for the existence of such a control mechanism during postnatal hair growth and development, we examined *Hoxc13* RNA and LZ-GC13 β-gal expression in sectioned skin of 5-day-old normal and GC13 mutant mice. While the in situ hybridization data clearly indicated substantially increased levels of *Hoxc13* expression in the upper bulb and lower shaft regions of GC13 versus normal anagen hair follicles (Fig. 3C), the levels of LZ-GC13 reporter gene activity in the same regions presented the reverse situation, i.e. LZ-GC13 expression was drastically reduced in LZ-GC13/GC13 mutant compared with normal hair follicles in LZ-GC13 mice (Fig. 3D). Combined, these data suggest employment of a negative autoregulatory feedback mechanism that, either directly or indirectly, controls *Hoxc13* expression levels during development of both axial skeleton and hair follicles.

Hyperproliferation of keratinocytes in skin of GC13 mice

To examine whether the enlargement of hair follicles and the thickening of the epidermis in mutant skin reflect changes in the proliferation rates of precursor cells, we performed bromodeoxyuridine (BrdU) assays with 2-day-old normal and mutant skin. The results showed an increase in the number of

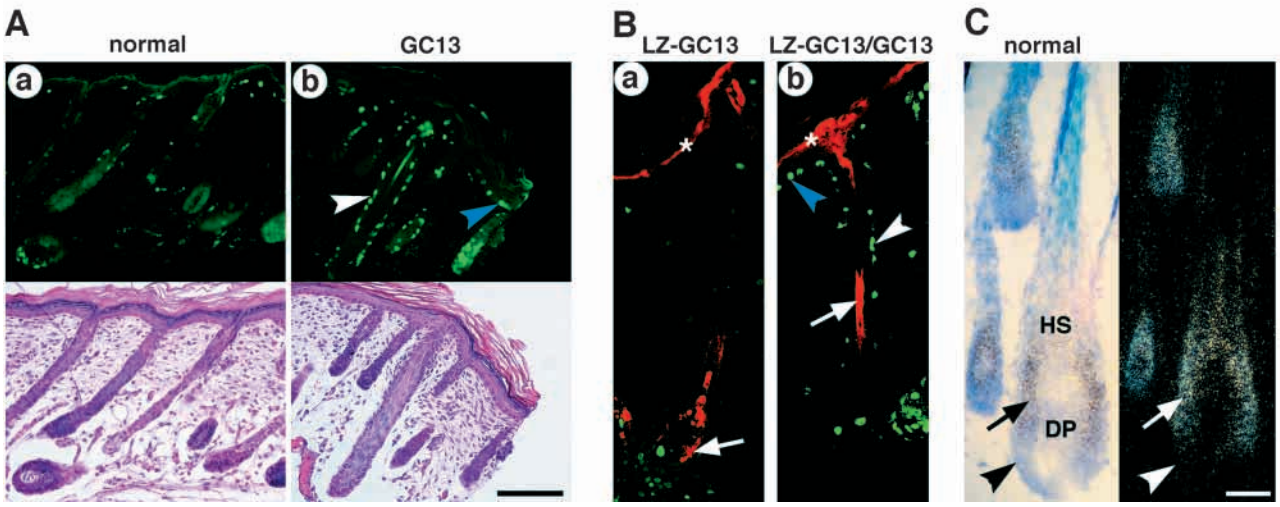

Fig. 4. Keratinocyte hyperproliferation and *Hoxc13* expression in differentiating keratinocytes. (A) BrdU-labeling of 2-day-old normal (a) and GC13 mutant (b) skin, as visualized by fluorescence microscopy of 7 μm sagittal sections (top); bottom panels show the same sections counterstained with Hematoxylin and Eosin. Note increased number of BrdU-labeled nuclei in outer root sheath (white arrowhead) and in basal epidermal layer (blue arrowhead) in mutant skin (b). (B) Spatial relationship between LZ-GC13 expression and keratinocyte hyperproliferation was revealed by double-fluorescence microscopy of 10 μm skin sections derived from 2-day-old normal LZ-GC13 (a) and mutant LZ-GC13/GC-13 (b) pups using rhodamine-conjugated anti-β-gal and fluorescin-conjugated anti-BrdU antibodies; note non-overlap between LZ-GC13-expressing (red-labeled follicular cells marked by white arrows) and proliferating keratinocytes in normal (a) and mutant (b) hair follicles; blue arrowhead in b points to increased anti-BrdU-labeling of basal epidermal keratinocytes; white asterisks in a,b indicate nonspecific labeling of the squamous epidermis with anti-β-gal antibodies. (C) *Hoxc13* in situ hybridization signals in bulb and lower shaft region of anagen hair follicle in 5-day-old normal skin section counterstained with Giemsa; specific signal is detectable as accumulation of silver grains under bright- (dark grains in left-hand panel) and darkfield (bright grains in right-hand panel) illumination over differentiating keratinocytes in the upper bulb region (arrows) and lower hairshaft (HS); no expression is detectable in lower bulb regions (arrowheads) and in dermal papilla (DP). Scale bars: 100 μm in A,C.

BrdU-labeled nuclei in the ORS of mutant hair follicles and in the basal layer of mutant epidermis (Fig. 4A), regions that appear to exclude *Hoxc13* expression, as determined by X-gal staining of skin from 2-day-old (data not shown) and 5-day-old LZ-GC13 mice (Fig. 3D), as well as by in situ hybridization in 5-day-old normal and GC13 mutant skin (Figs 3C, 4C). To examine more directly whether *Hoxc13* is expressed in proliferating or differentiating keratinocytes, we performed double-immunofluorescence analysis on BrdU-labeled sections of 2-day-old normal LZ-GC13 and mutant LZ-GC13/GC13 skin by using anti-BrdU and anti-β-gal antibodies (Fig. 4B, parts a,b). As the results show no overlap between β-gal-positive and BrdU-labeled cells, we can conclude that *Hoxc13* is expressed in differentiating keratinocytes and that the hyperproliferation of both follicular and epidermal keratinocytes in GC13 mutant skin is an intercellular response to *Hoxc13* overexpression in differentiating cells. The GC13 mutant hair phenotype is thus directly linked to *Hoxc13* overexpression in differentiating keratinocytes of the upper bulb and lower shaft regions of the hair follicle, regions that are known to express hair-specific keratin genes including intermediate filament- (IF) and KAP-encoding genes (reviewed by Fuchs, 1995; Powell and Rogers, 1997).

Identification of hair-specific genes as Hoxc13 downstream targets

As a first step toward defining the molecular mechanisms that underlie the pathological changes observed in GC13 mutant skin, we screened for differentially expressed genes in skin of 5 d GC13 mice. We chose this developmental stage because the more advanced pathological manifestations seen at later stages could result in secondary and increasingly nonspecific changes in gene expression, whereas earlier skin contains only a small fraction of fully differentiated hair follicles (Paus et al., 1999). Using a strategy based on suppression subtractive hybridization (SSH) (Diatchenko et al., 1996; Tkatchenko et al., 2000), we isolated 74 potentially differential cDNA clones. Reverse northern quantitative hybridization of these cDNAs using complex cDNA probes (Fig. 5A), identified a total of four upregulated and 25 downregulated sequences (Fig. 5B). The overexpressed cDNAs corresponded to four known genes that included, most conspicuously, keratin complex 2 gene 1 (K1), whose overexpression in mutated form in transgenic mice reproduced features of epidermolytic hyperkeratosis (Bickenbach et al., 1996), a skin disorder with similarities to the one observed here. Of apparent relevance is also the overexpression of a member of the 14-3-3 protein gene family. The 14-3-3 proteins are known to play a role in keratinocyte differentiation and proliferation and interact with K8 and K18 keratins in a cell-cycle- and phosphorylation-dependent manner (Liao and Omary, 1996).

Remarkably consistent with a *Hoxc13* role in hair follicle development and hair growth is our finding that the 25 downregulated cDNAs included five sequences that corresponded to previously known hair-specific KAP-encoding genes, as well as nine novel sequences that were found to have closest similarities to KAP genes of the high glycine tyrosine (HGTp) class, including the murine *HGTpII.1* (*Krtap6-1* – Mouse Genome Informatics) and *HGTpI-alpha* (*Krtap8-2* – Mouse Genome Informatics; Aoki et al., 1997) identified here

A

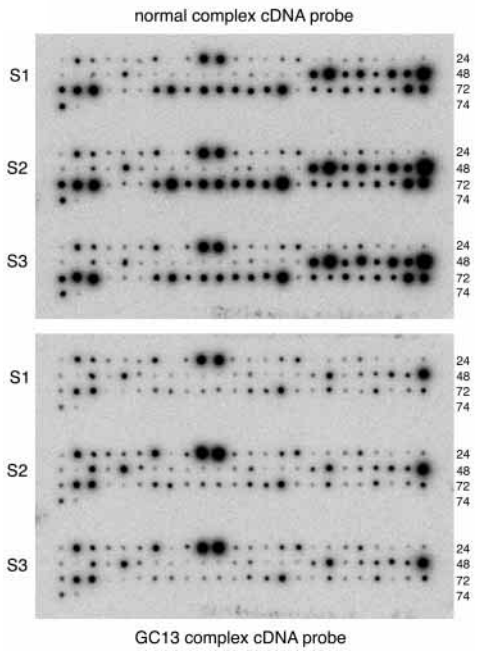

B

Array No.	Clone	Identity	N/GC13	s.d.
2	GC13A19	integral membrane protein 2B (Itm2b)	0.63	0.04
7	GC13C22	cysteine proteinase inhibitor MS3 (mouse stefin 3)	0.44	0.07
11	GC13I17	keratin complex 2 gene 1 (Krt2-1)	0.49	0.05
29	GC13J24	14-3-3 protein, β subtype	0.66	0.17
41	NA7	agouti-related protein	13.24	0.48
42	NB14	high-glycine/tyrosine protein (HGTp) type II.1	9.34	0.77
43	NB18	high-glycine/tyrosine protein (HGTp) type I alpha	10.44	0.09
44	ND1	keratin-associated protein Pmg-2	15.02	0.92
45	ND19	keratin-associated protein Pmg-1	2.54	0.14
46	NE3	keratin complex 1 gene 1 (Krt1-1)	6.63	0.30
47	NJ3	hacl-1	5.91	0.49
48	NM1	type II cytokeratin	3.23	0.26
73	NO20	orphan G-protein coupled receptor (Gprc5d)	2.88	0.05
49	NA15	keratin-associated protein 16-3 (Krtap16-3) (novel)	6.62	0.92
51	NA24	keratin-associated protein 16-8 (Krtap16-8) (novel)	4.69	1.23
53	NC9	novel	1.71	0.06
55	NC18	novel	3.89	0.22
56	ND4	keratin-associated protein 16-1 (Krtap16-1) (novel)	10.16	0.57
57	ND5	keratin-associated protein 16-4 (Krtap16-4) (novel)	5.33	0.37
58	ND22	keratin-associated protein 16-5 (Krtap16-5) (novel)	10.42	1.34
59	NE7	keratin-associated protein 16-6 (Krtap16-6) (novel)	7.95	1.34
60	NE10	keratin-associated protein 16-2 (Krtap16-2) (novel)	9.49	0.51
61	NE15	keratin-associated protein 16-7 (Krtap16-7) (novel)	3.88	0.33
65	NI18	novel	6.51	1.18
67	NJ22	novel	8.11	1.08
68	NK1	novel	3.93	0.08
69	NL14	novel	2.37	0.07
70	NL15	novel	5.51	0.58
71	NM20	keratin-associated protein 16-9 (Krtap16-9) (novel)	21.54	2.14

Fig. 5. Identification of genes differentially expressed in GC13 skin. (A) Reverse northern quantitative hybridization. 30 ng of each of 74 plasmid DNAs were spotted in triplicate on two filters hybridized in parallel with normal and GC13 skin complex cDNA probes. Washed filters were exposed to an imaging plate and scanned images (STORM 860 scanner, Molecular Dynamics) analyzed and quantified using Image Quant 1.0 software. Resulting tables containing intensities of all spots were exported to Excel and further calculations were performed using Excel worksheet. S1, series 1; S2, series 2; S3, series 3. (B) List of genes differentially expressed in GC13 skin. Upregulated and downregulated genes in GC13 skin are indicated by showing corresponding ratios of expression, N/GC13, in red and green, respectively. Downregulated KAP genes mapped to mouse chromosome 16 (see Fig. 6B) are shown in blue. The greatest spot-to-spot variation in the intensity of hybridization signal observed for the same cDNA was 1.21±0.08 (mean±s.d., n=6); therefore, only differences greater or equal to 1.5-fold are significant and shown in the table. Array No., cDNA array coordinate; N/GC13, mean values for the differences in expression (normal versus GC13); s.d., standard deviation (n=9).

(Figs 5B, 6A). We propose to designate the nine novel HGTp-type KAP genes *Krtap16-1* to *Krtap16-9* because our phylogenetic tree and genomic mapping analysis indicate that they belong to a novel cluster of structurally similar genes (see below). The previously reported expression patterns of the identified known KAP genes, *HGTpII.1* and *HGTpI-alpha* (Aoki et al., 1997), *Pmg1* (*Krtap14* – Mouse Genome Informatics), *Pmg2* (*Krtap15* – Mouse Genome Informatics; Kuhn et al., 1999) and *Hacl1* (*Krtap11-1* – Mouse Genome Informatics; Huh et al., 1994), as well as the IF keratin gene *Krt1-1* (Bertolino et al., 1988), extensively overlap with the GC13 transgene expression pattern in differentiating keratinocytes of the hairshaft (Figs 3, 4). This, combined with the high levels of downregulation of between 2.5- and 21.5-fold for this subgroup, suggests that these genes are downstream targets of Hoxc13.

Apart from the keratin and KAP genes, a conspicuous member of the group of repressed genes is agouti-related protein (*Agrp*), whose 13-fold downregulation might be of relevance to the overall smaller stature and reduced body weight, as well as the skin phenotype of GC13 mice. Like its close structural relative, agouti protein, Agrp is a paracrine signaling molecule that has been implicated in the control of body weight as a hypothalamic Mc4r melanocortin receptor antagonist, as evidenced by obesity in transgenic mice that ubiquitously overexpressed *Agrp* (Ollmann et al., 1997). Recent findings of expression in numerous tissues in chicken, including skin, could suggest a role for Agrp in regulating peripheral melanocortin systems as well (Takeuchi et al., 2000). However, further information about *Agrp* expression pattern and function in skin will be required for understanding the significance of its downregulation in GC13 skin.

Genomic mapping of a novel KAP gene cluster controlled by Hoxc13

Insight into the structural and phylogenetic relationships among the identified KAP-related cDNAs was gained by generating a phylogenetic tree using a multiple sequence alignment program (see Materials and Methods). The data revealed that the nine novel KAP cDNAs were structurally more related to each other and to *HGTpII.1* and *HGTpI-alpha* than to the remaining known KAP genes identified (Fig. 6A), thus suggesting that they correspond to members of a new distinct subgroup which we propose to designate *Krtap16-n*, according to human genome organization (HUGO) keratin gene nomenclature (http://www.gene.ucl.ac.uk/). Furthermore, our sequence comparison of the nine novel KAP-related cDNA sequences, *Krtap16-1* to *Krtap16-9*, against public databases revealed highest similarity to a previously unidentified cluster of KAP-related sequences located in the human chromosome

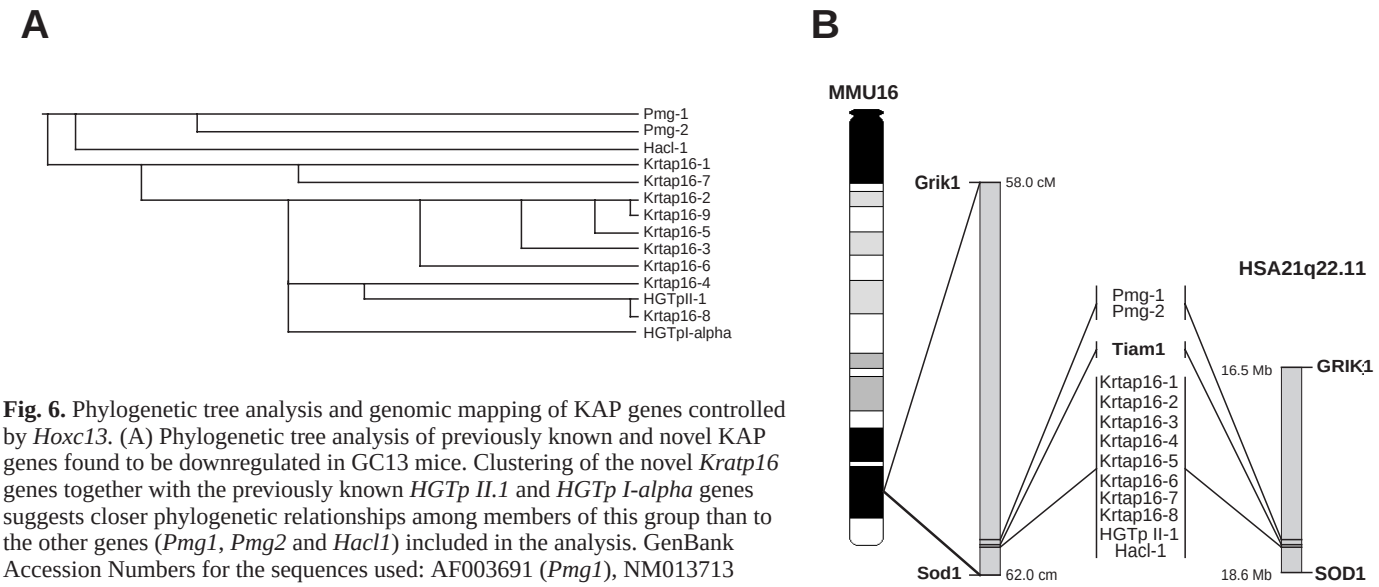

Fig. 6. Phylogenetic tree analysis and genomic mapping of KAP genes controlled by *Hoxc13*. (A) Phylogenetic tree analysis of previously known and novel KAP genes found to be downregulated in GC13 mice. Clustering of the novel *Kratp16* genes together with the previously known *HGTp II.1* and *HGTp I-alpha* genes suggests closer phylogenetic relationships among members of this group than to the other genes (*Pmg1*, *Pmg2* and *Hacl1*) included in the analysis. GenBank Accession Numbers for the sequences used: AF003691 (*Pmg1*), NM013713 (*Pmg2*), U03686 (*Hacl1*), D86420 (*HGTp II.1*), D86422 (*HGTp I-alpha*), AF345291 (*Krtap16-1*), AF345292 (*Krtap16-2*), AF345293 (*Krtap16-3*), AF345294 (*Krtap16-4*), AF345295 (*Krtap16-5*), AF345296 (*Krtap16-6*), AF345297 (*Krtap16-7*), AF345298 (*Krtap16-8*), AF345299 (*Krtap16-9*). (B) Schematic representation of genomic mapping results: KAP genes (shown in regular type) analyzed here map between the two distal markers *Grik1* and *Sod1* (shown in bold type) on mouse chromosome 16 (MMU16), a region of conserved linkage with human chromosome HSA21q22.11 region. Novel KAP genes *Krtap16-1* to *Krtap16-8* cluster together with *HGTpII.1* and *Hacl-1*, distal to *Tiam1* and occupy a conserved position in the HSA21q22.11 region as indicated; the more distantly related *Pmg1* and *Pmg2* genes map proximal to *Tiam1*.

21q22.11 region (Hattori et al., 2000). As this region is of conserved linkage with the distal region of mouse chromosome 16, we predicted clustering of the *Krtap16* genes in that part of the mouse genome. This assumption was confirmed by mapping *Krtap16-1* to *Krtap16-8* between the two distal markers *Tiam1* and *Sod1* on mouse chromosome 16 using a mouse/hamster radiation hybrid panel (Fig. 6B). Of the known KAP genes identified as presumptive Hoxc13 targets, we mapped the *HGTpII.1* and *HGTpI-alpha*, which are structurally similar to the *Krtap16* genes, to the same region, as well as the more distantly related *Hacl-1*. However, the structurally distinct *Pmg1* and *Pmg2* genes, which are known to be closely linked to each other (Kuhn et al., 1999), were mapped proximal to the *Tiam1* marker (Fig. 6B).

DISCUSSION

Our data show that increased levels of *Hoxc13* expression in hair follicles during pre- and postnatal development cause severe hair and skin defects including alopecia and a progressive hyperproliferative disorder resembling ichthyosis. The hair phenotype is similar to the hair growth defects observed recently in *Hoxc13*-targeted mice (Godwin and Capecchi, 1998), thus suggesting that the hair defects exhibited by our two independent GC13 transgenic strains are *Hoxc13* specific. Accordingly, one can conclude that the level of *Hoxc13* expression is a crucial parameter for proper hair growth and development. These results support the concept of antipodal regulation of Hox genes stating that overexpression and underexpression may result in similar phenotypic changes (Pollock et al., 1992). Apparently, this concept is of relevance also for other developmental regulatory genes encoding transcription factors as demonstrated by the influence of human *PAX6* gene dose on eye development in transgenic mice (Schedl et al., 1996). In that case, overexpression on wild-type background caused distinct eye abnormalities similar to the murine *Pax6* mutant phenotype small eye.

Negative feedback regulation of Hoxc13 expression

The apparent great sensitivity of certain cell populations to changes in the expression levels of crucial transcriptional regulators suggests the existence of control mechanisms capable of providing stable physiological expression levels. Useful models for such mechanisms in mammalian systems might be synthetic gene circuits engineered in *E. coli*, which facilitate examining the behavior of individual system components quantitatively and, thus, allow to make predictions about system stability (Gardner and Collins, 2000). Following this approach by using circuits that consisted of a regulator and repressor modules has demonstrated that negative feedback can increase system stability by dramatically reducing variability in gene expression (Becskei and Serrano, 2000), an essential requirement for homeostasis. In view of these findings, our own data that indicate involvement of a negative feedback mechanism in the control of *Hoxc13* expression levels provide significant new insight into the regulation of a Hox gene, in this case a gene that plays a pivotal role in hair growth and development. As both over- and underexpression of individual members of a group of genes encoding structural components of hair, i.e. the hair keratin genes, has been shown to result in severe hair growth abnormalities including brittleness and hair loss (e.g. Powell and Rogers, 1990; Schlake et al., 2000), one may conclude that their normal expression levels need to be well balanced and tightly controlled. Presumably, this control will not tolerate wide fluctuations in the expression levels of

upstream transcriptional regulators, a group of genes that, as we have shown here, includes *Hoxc13*.

The sequential activation of Hox genes in the embryo occurs in distinct, though overlapping, anterior-posterior (A/P) expression domains whose order is co-linear with the map positions of the corresponding Hox genes in their transcriptionally unipolar clusters (Krumlauf, 1994). Accordingly, genes located at the 3′ end of a Hox cluster will become activated first and occupy the most anterior domain, while subsequent expression of genes located further 5′ will become increasingly posteriorly restricted.

Within their initial A/P expression domains, each Hox gene is typically active in cells of different morphogenetic lineages, and thus may contribute to the formation of various organ systems (Krumlauf, 1994). During subsequent stages of embryogenesis, these initial expression domains undergo dynamic changes and many Hox genes continue to be active in a wide variety of tissues during postnatal development and adulthood. Orchestrating these complex patterns of gene activity requires elaborated regulatory circuitries.

Although little is known about mechanisms controlling quantitative levels of expression, considerable insight has been gained into qualitative and temporal control mechanisms. Accordingly, translocation experiments within the Hoxd cluster that involve placement of anteriorly expressed genes into the genomic environment of 'posterior' genes, suggest that, within cluster context, the timepoint of activation is not autonomously regulated by the control elements specific for the translocated gene, but largely determined by its relative proximity to the 5′ end of its cluster (van der Hoeven et al., 1996). Furthermore, deletion of genomic segments upstream of the *Hoxd* cluster revealed that the successive 3′→5′ activation is regulated by control elements located upstream of the cluster, which apparently mediate a silencing mechanism (Kondo and Duboule, 1999). Release of this silencing mechanism is believed to render downstream target genes progressively accessible for transcription (Kmita et al., 2000), involving the function of multiple and dispersed local control elements that regulate a multitude of subsequent temporal and regional specificities in expression (Krumlauf, 1994). Some elements have been shown to function as components of positive auto- and crossregulatory circuits which are believed to be essential for maintaining Hox gene activity (e.g. Gould et al., 1997), whereas repressor elements might be required for the refinement of expression boundaries (e.g. Bieberich et al., 1990; Nonchev et al., 1997). Although this has not yet been demonstrated, we speculate that some of these inhibitory elements might play a role in stabilizing quantitative levels of expression as system components in negative feedback circuits, and *Hoxc13* might serve as a paradigm for elucidating these quantitative regulatory mechanisms.

Identification of Hoxc13 downstream target genes

A prerequisite for understanding the complex patterning functions of Hox genes is to identify their downstream target genes. Although the number of Hox targets in *Drosophila* alone has been estimated to range in the thousands (Biggin and McGinnis, 1997), to date only relatively few presumptive downstream genes have been isolated in both flies and vertebrates. About two to three dozen *Drosophila* Hox targets have been isolated by using various approaches (reviewed by Graba et al., 1997), including genetic studies (Bienz, 1994), enhancer trapping (Wagner-Bernholz, 1991), immunoprecipitation of in vivo formed Hox protein/DNA complexes (e.g. Gould et al., 1990; Graba et al., 1992), cDNA subtraction (Feinstein et al., 1997) and the selection of genomic fragments that confer reporter gene activity on Hox gene expression in yeast cells (Mastick et al., 1995). Only a handful of mammalian Hox downstream targets, including the mouse homolog of the *Drosophila* tumor suppressor gene *lethal(2)giant larvae* (Tomotsune et al., 1993), *Ncam* (Jones et al., 1993), the human *Lamin B2* DNA replication origin (de Stanchina et al., 2000), the cyclin-dependent kinase inhibitor *p21* (Bromleigh and Freedman, 2000) and the tumor suppressor gene *p53* (Raman et al., 2000) have been identified by immunoprecipitation and a combination of in vivo and in vitro protein/DNA-binding methods. For the majority of these fly and mammalian downstream genes, it can currently not be ascertained whether they are being directly or indirectly targeted by Hox proteins.

We have used suppression subtractive hybridization (SSH) of cDNAs (Diatchenko et al., 1996) combined with reverse northern quantitative hybridization to identify genes that are differentially expressed in 5-day-old postnatal skin of GC13 mutant mice. Our approach is conceptually similar to a more conventional cDNA subtraction successfully pursued by Feinstein and co-workers that resulted in the isolation of Ubx target genes in *Drosophila* (Feinstein et al., 1995). In that case, cDNAs differentially expressed in fly embryos ubiquitously expressing *Ubx* upon heat shock induction were enriched by subtraction and used as a complex probe for screening a genomic library, thus isolating five previously known genes activated by Ubx.

Apart from using a different animal model system, our screen differs in several important ways from those studies. First, in contrast to other subtractive hybridization methods, which usually favour enrichment of highly expressed mRNAs, a key feature of SSH is equalization of enrichment levels among highly, moderately and rarely expressed messages; this greatly increases the overall efficiency of the screening process. Second, instead of ubiquitously expressing *Hoxc13*, overexpression was restricted to the normal activity domains of this gene; this strategy should minimize the risk of isolating presumptive targets that might be irrelevant for the normal function of this gene. Third, our screen aimed at identifying unregulated, as well as downregulated targets. As our results indicate, the latter group is highly relevant, as it comprises by far most of the downstream genes identified. This raises the question of to what extent this particular outcome could have been predicted.

To answer this question, it is useful to consider two competing models for the role of DNA binding of Hox proteins in their functional activity and specificity, as proposed by Biggin and McGinnis (Biggin and McGinnis, 1997). The first predicts that sequence-specific binding of Hox proteins requires cooperative interactions with co-factors such as Pbx and Exd. This so called 'co-selective binding model' is supported by data that show distinct DNA-binding specificities for different Hox protein/Pbx complexes (Pöpperl et al., 1995; Mann and Chan, 1996). In contrast, the second model suggests that most Hox proteins bind independently (without prior heteroduplex formation with co-factors) to a large number of binding sites that contain a simple core recognition sequence

where they principally act as repressors. According to this 'widespread binding model', DNA-bound Hox protein will be transformed from transcriptional repressor to activator only upon secondary interaction with specific co-factor(s). Under the premise of increased ratios of Hoxc13 protein/co-factor(s) in our GC13 mice, this model would predict a shift towards a presumptive transcriptional repressor function of Hoxc13 and thus a downregulation of target genes, a speculation that is consistent with our data. As this model is based on direct Hox protein-DNA interactions, one might further conclude that most of the downregulated genes identified here are direct transcriptional targets for Hoxc13. However, invoking the 'co-selective binding model' for predicting the effects of excessive Hoxc13 protein under the assumption of limited co-factor supply might favor a more neutral outcome with respect to the activation or repression of presumptive targets, because Hox/Pbx complexes have been shown to be capable of acting either as transcriptional activators or repressors depending on association with additional co-factors (Saleh et al., 2000). Furthermore, one might predict indirect effects due to generally reduced availability of presumptive co-factors shared among Hoxc13 and other Hox proteins, i.e. excessive Hoxc13 might act as a co-factor sink.

Clustering of realisator genes

KAP genes form by far the largest group of presumptive Hoxc13 targets identified in this screen, i.e. 14 out of a total of 29 genes, including nine that have been classified as novel KAPs. All of these KAPs are downregulated by between approx. 2.5-fold (*Pmg1*) to more than 20-fold (*Krtap 16-9*) when compared with normal levels (Fig. 5A,B). KAP gene products presumably are involved in alignment and lateral crosslinking of keratin intermediate filaments (IFs), thus playing an important role in epidermal and follicular keratinocyte differentiation (Powell and Rogers, 1997; Fuchs, 1995). Structural similarities allow us to distinguish several different groups of KAPs whose distinct expression patterns reflect the functional diversity among keratinocytes. While certain structurally unique epidermal KAPs, such as fillagrin and loricrin, are encoded by spliced transcripts (Markova et al., 1993; Rothnagel et al., 1994), all follicular KAPs identified to date appear to be encoded by small intron-less genes (Powell and Rogers, 1997). Based on their amino acid composition, the latter group has been classified into high sulfur proteins (containing up to 40% cysteine), and the high-glycine/tyrosine (HGT) proteins (Powell et al., 1991; Powell and Rogers, 1997). Both classes include several subfamilies summarily designated as Krtaps (keratin-associated proteins) followed by a number specifying the family and its individual member (HUGO keratin gene nomenclature; http://www.gene.ucl.ac.uk/users/hester/krt.html). Accordingly, we propose that the nine novel HGTp-type KAP genes be designated individually as *Krtap16-1* to *Krtap16-9*, as they form a 16th group of structurally distinct genes, located in a novel cluster in a distal region of mouse chromosome 16 – a region syntenic to human chromosome 21q22.11. Interestingly, at least one additional KAP gene cluster and several individual KAP genes in mouse, cattle and sheep have been mapped to different genomic regions of synteny with human chromosome 21 including, among others, a cluster of high sulfur KAP genes of the murine *Krtap12* group on mouse chromosome 10 (HSA21q22.3; Cole and Reeves, 1998), and the HGTp-type *Krtap8* gene on bovine chromosome 1 (HSA21q22.1; Harlizius et al., 1997).

The conserved genomic organization and clustering of KAP genes may reflect a constraining force of relevance for coordinate expression. This view is consistent with the sequential activation of keratin and KAP genes in distinct subpopulations of keratinocytes during follicle differentiation (Powell and Rogers, 1997). Accordingly, the first class of genes expressed is the group of IF keratin genes, followed by the HGTp class and later by high sulfur protein genes. Furthermore, expression data obtained with several similar HGTp-type KAPs indicate temporal progression of activation of members of the same subgroup (Aoki et al., 1997), i.e. genes that (according to our genomic mapping results) cluster closely together with the novel *Krtap16* genes. This apparent sequential activation of KAP genes is reminiscent of the Hox gene activation patterns, and once the HGTp-type *Krtap16* gene cluster has been characterized in more detail, it will be of great interest to see whether spatio-temporal expression patterns of its members occurs in a co-linear fashion with respect to their map position – a feature currently unique to the Hox clusters (Krumlauf, 1994).

It has been proposed that Hox genes coordinate the activities of thousands of realisator genes in a concerted fashion, because independent control of the realisators would result in chaotic development (Gehring, 1987). One would predict that during evolution this logistical demand has been coped with by clustering of functionally similar realisator genes. Our identification of such a realisator gene cluster controlled by Hoxc13 supports this concept and provides an experimental system for studying the mechanisms of its regulation.

The authors thank R. Lee, G. McPhillips, C. Moskos and M. Romano for technical support; C. Little, D. Hazen-Martin and J. Maize for advice; and T. Hsu, W. McGinnis, D. Spyropoulos, K. Stenn and D. Watson for comments on the manuscript. The work was supported by funds from the RGK foundation, and National Institute of Health grants GM43334-10 and AR47204-01.

REFERENCES

Aoki, N., Ito, K. and Ito, M. (1997). Isolation and characterization of mouse high-glycine/tyrosine proteins. *J. Biol. Chem.* **272**, 30512-30518.

Awgulewitsch, A. and Utset, M. F. (1991). In *Methods in Nucleic Acids Research* (ed. J. D. Karem, L. Chao and G. Warr), pp. 359-375. Boca Raton, FL: CRC Press.

Becskei, A. and Serrano, L. (2000). Engineering stability in gene networks by autoregulation. *Nature* **405**, 590-593.

Bertolino, A. P., Checkla, D. M., Notterman, R., Sklaver, I., Schiff, T. A., Freedberg, I. M and DiBona, G. J. (1988). Cloning and characterization of a mouse type I hair keratin cDNA. *J. Invest. Dermatol.* **91**, 541-546.

Bickenbach, J. R., Longley, M. A., Bundman, D. S., Dominey, A. M., Bowden, P. E., Rothnagel, J. A. and Roop, D. R. (1996). A transgenic model that recapitulates the clinical features of both neonatal and adult forms of the skin disease epidermolytic hyperkeratosis. *Differentiation* **61**, 129-139.

Bieberich, C. J., Utset, M. F., Awgulewitsch, A. and Ruddle, F. H. (1990). Evidence for positive and negative regulation of the Hox3.1 gene. *Proc. Natl. Acad. Sci. USA* **87**, 8462-8466.

Bienz, M. (1994). Homeotic genes and positional signalling in the Drosophila viscera. *Trends Genet.* **10**, 22-26.

Biggin, M. D. and McGinnis, W. (1997). Regulation of segmentation and segmental identity by Drosophila homeoproteins: the role of DNA binding in functional activity and specificity. *Development* **124**, 4425-4433.

Bromleigh, V. C. and Freedman, L. P. (2000). p21 is a transcriptional target

of HOXA10 in differentiating myelomonocytic cells. *Genes Dev.* **14**, 2581-2586.

Capecchi, M. R. (1997). *Hox* genes and mammalian development. *Cold Spring Harb. Symp. Quant. Biol.* **62**, 273-281.

Chang, P. Y., Kozono, T., Chida, K., Kuroki, T. and Huh, N. (1998). Differential expression of Hox genes in multistage carcinogenesis of mouse skin. Biochem. *Biophys. Res. Comm.* **248**, 749-752.

Cole, S. E. and Reeves, R. H. (1998). A cluster of keratin-associated proteins on mouse chromosome 10 in the region of conserved linkage with human chromosome 21. *Genomics* **54**, 437-442.

de Stanchina, E., Gabellini, D., Norio, P., Giacca, M., Peverali, F. A., Riva, S., Falaschi, A. and Biamonti, G. (2000). Selection of homeotic proteins for binding to a human DNA replication origin. *J. Mol. Biol.* **299**, 667-680.

Diatchenko, L., Lau, Y. F., Campbell, A. P. Chenchik, A., Maquadam, F., Huang, B., Lukyanov, S., Lukyanov, K., Gurskaya, N., Sverdlov, E. D. and Siebert, P. D. (1996). Suppression subtractive hybridization: a method for generating differentially regulated or tissue-specific cDNA probes and libraries. *Proc. Nat. Acad. Sci. USA* **93**, 6025-6030.

Feinstein, P. G., Kornfeld, K., Hogness, D. and Mann, R. S. (1995). Identification of homeotic target genes in Drosophila melanogaster including nervy, a proto-oncogene homologue. *Genetics* **140**, 573-586.

Fuchs, E. (1995). Keratins and the skin. *Annu. Rev. Cell Dev. Biol.* **11**, 123-153.

Garcia-Bellido, A. (1975). Genetic control of wing disc development in Drosophila. *Ciba Found. Symp.* **29**, 161-178.

Gardner, T. S. and Collins, J. J. (2000). Neutralizing noise in gene networks. *Nature* **405**, 520-521.

Gehring, W. J. (1987). Homeo boxes in the study of development. *Science* **236**, 1245-1252.

Godwin, A. R. and Capecchi, M. R. (1998). Hoxc13 mutant mice lack external hair. *Genes Dev.* **12**, 11-20.

Gould, A. P., Brookman, J. J., Strutt, D. I. and White, R. A. H. (1990). Targets for homeotic gene control in Drosophila. *Nature* **348**, 308-312.

Gould, A., Morrison, A., Sproat, G., White, R. A. H. and Krumlauf, R. (1997). Positive cross-regulation and enhancer sharing: two mechanisms for specifying overlapping Hox expression patterns. *Genes Dev.* **11**, 900-913.

Graba, Y., Aragnol, D., Laurenti, P., Garzino, V., Charmot, D., Berenger, H. and Pradel, J. (1992). Homeotic control in Drosophila: the scabrous gene is and in vivo target of Ultrabithorax proteins. *EMBO J.* **11**, 3375-3384.

Graba, Y. Aragnol, D. and Pradel, J. (1997). Drosophila Hox complex downstream targets and the function of homeotic genes. *BioEssays* **19**, 379-388.

Greer, J. M., Puetz, J., Thomas, K. R. and Capecchi, M. R. (2000). Maintenance of functional equivalence during paralogous Hox gene evolution. *Nature* **403**, 661-664.

Harlizius, B., Tammen, I., Eichler, K., Eggen, A. and Hetzel, D. J. (1997). New markers on bovine chromosome 1 are closely linked to the polled gene in Simmenthal and Pinzgauer cattle. *Mamm. Genome* **8**, 255-257.

Hattori, M., Fujiyama, A., Taylor, T. D., Watanabe, H., Yada, T., Park, H.-S., Toyada, A., Ishii, K., Totoki, Y., Choi, D.-K., et al. (2000). The DNA sequence of human chromosome 21. *Nature* **405**, 311-319.

Hérault, Y., Hraba-Renevey, S., van der Hoeven, F. and Duboule, D. (1996). Function of the Evx-2 gene in the morphogenesis of vertebrate limbs. *EMBO J.* **15**, 6727-6738.

Hogan, B. L. M., Beddington, R., Constantini, F. and Lacy, E. (1994). *Manipulating The Mouse Embryo: A Laboratory Manual*. 2nd edn. New York: Cold Spring Harbor Laboratory Press.

Huh, N., Kashiwagi, M., Konishi, C., Hashimoto, Y., Kohno, Y., Nomura, S. and Kuroki, T. (1994). Isolation and characterization of a novel hair follicle-specific gene, Hacl-1. *J. Invest. Dermatol.* **102**, 716-720.

Jones, F. S., Holst, B. D., Minowa, O., DeRobertis, E. M. and Edelman, G. M. (1993). Binding and transcriptional activation of the promoter for the neural cell adhesion molecule by HoxC6 (Hox-3.3). *Proc. Natl. Acad. Sci. USA* **90**, 6557-6561.

Kmita, M., van der Hoeven, F., Zákány, J., Krumlauf, R. and Duboule, D. (2000). Mechanisms of Hox gene colinearity: transposition of the anterior Hoxb1 gene into the posterior HoxD complex. *Genes Dev.* **14**, 198-211.

Kondo, T. and Duboule, D. (1999). Breaking colinearity in the mouse HoxD complex. *Cell* **97**, 407-417.

Kozak, M. (1983). Comparison of initiation of protein synthesis in procaryotes, eucaryotes, and organelles. *Microbiol. Rev.* **47**, 139-45.

Krumlauf, R. (1994). Hox genes in vertebrate development. *Cell* **78**, 191-201.

Kuhn, F., Lassing, C., Range, A., Mueller, M., Hunziker, T., Ziemiecki, A. and Andres, A.-C. (1999). Pmg-1 and Pmg-2 constitute a novel family of KAP genes differentially expressed during skin and mammary gland development. *Mech. Dev.* **86**, 193-196.

Liao, J. and Omary, M. B. (1996). 14-3-3 proteins associate with phosphorylated simple epithelial keratins during cell cycle progression and act as a solubility cofactor. *J. Cell. Biol.* **133**, 345-357.

Mann, R. S. and Chan, S.-K. (1996). Extra specificity from extradenticle: the partnership between HOX and PBX/EXD homeodomain proteins. *Trends Genet.* **12**, 258-262.

Markova, N. G., Marekov, L. N., Chipev, C. C., Gan, S.-Q., Idler, W. W. and Steinert, P. M. (1993). Profillagrin is a major epidermal calcium-binding protein. *Mol. Cell. Biol.* **13**, 613-625.

Mastick, G. S., McKay, R., Oligino, T., Donovan, K., Lopez, A. J. (1995). Identification of target genes regulated by homeotic proteins in Drosophila melanogaster through genetic selection of Ultrabithorax protein-binding sites in yeast. *Genetics* **139**, 349-363.

Mortlock, D. P., Post, L. C. and Innis, J. W. (1996). The molecular basis of hypodactyly (Hd): a deletion in Hoxa13 leads to arrest of digital arch formation. *Nat. Genet.* **13**, 284-289.

Nonchev, S., Maconochie, M., Gould, A., Morrison, A. and Krumlauf, R. (1997). Cross-regulatory interactions between Hox genes and the control of segmental expression in the vertebrate central nervous system. *Cold Spring Harb. Symp. Quant. Biol.* **62**, 313-323.

Ollmann, M. M., Wilson, B. D., Yang, Y.-K, Kerns, J. A., Chen, Y., Gantz, I. and Barsh, G. S. (1997). Antagonism of central melanocortin receptors in vitro and in vivo by Agouti-related protein. *Science* **278**, 135-137.

Oro, A. E. and Scott, M. P. (1998). Splitting hairs: dissecting roles of signaling systems in epidermal development. *Cell* **95**, 575-578.

Papenbrock, T., Peterson, R. L., Lee, R. S., Hsu, T., Kuroiwa, A. and Awgulewitsch, A. (1998). Murine Hoxc9 gene contains a structurally and functionally conserved enhancer. *Dev. Dyn.* **212**, 540-547.

Paus, R., Müller-Röver, S., van der Veen, C., Maurer, M., Eichmüller, S., Ling, G., Hofmann, U., Foitzik, K., Mecklenburg, L., Hankjiski, B. (1999). A comprehensive guide for the recognition and classification of distinct stages of hair follicle morphogenesis. *J. Invest. Dermatol.* **113**, 523-532.

Peterson, R. L., Papenbrock, T., Davda, M. M. and Awgulewitsch, A. (1994). The murine Hoxc cluster contains five neighboring AbdB-related Hox genes that show unique spatially coordiated expression in posterior embryonic subregions. *Mech. Dev.* **47**, 253-260.

Pollock, R. A., Gilbert, J. and Bieberich, C. J. (1992). Altering the boundaries of Hox3.1 expression: evidence for antipodal regulation. *Cell* **11**, 911-932.

Pöpperl, H., Bienz, M., Studer, M., Chan, S.-K, Aparicio, S., Brenner, S., Mann, R. S. and Krumlauf, R. (1995). Segmental expression of Hoxb-1 is controlled by a highly conserved autoregulatory loop dependent upon exd/pbx. *Cell* **81**, 1031-1042.

Powell, B. C. and Rogers, G. E. (1990). Cyclic hair-loss and regrowth in transgenic mice overexpressing an intermediate filament gene. *EMBO J.* **9**, 1485-1493.

Powell, B. C., Nesci, A. and Rogers, G. E. (1991). Regulation of keratin gene expression in hair follicle differentiation. *Ann. New York Acad. Sci.* **642**, 1-20.

Powell, B. C. and Rogers, G. E. (1997). The role of keratin proteins and their genes in the growth, structure and properties of hair. In *Formation and Structure of Human Hair* (ed. P. Jolles, H. Zahn and H. Höcker), pp. 59-148. Basel, Switzerland: Birkhäuser Verlag.

Raman, V., Martensen, S. A., Reisman, D., Evron, E., Odenwald, W., Jaffee, E., Marks, J. and Sukumar, S. (2000). Compromised HOXA5 function can limit p53 expression in human breast tumours. *Nature* **405**, 974-978.

Rothnagel, J. A., Longley, M. A., Bundman, D. S., Naylor, S. L., Lalley, P. A., Jenkins, N. A., Gilbert, D. J., Copeland, N. G. and Roop, D. R. (1994). Characterization of the mouse loricrin gene: linkage with profillagrin and the flaky tail and soft coat mutant loci on chromosome 3. *Genomics* **23**, 450-456.

Saleh, M., Rambaldi, I., Yang, X. J. and Featherstone, M. S. (2000). Cell signaling switches HOX-PBX complexes from repressors to activators of transcription mediated by histone deacetylases and histone acetyltransferases. *Mol. Cell. Biol.* **20**, 8623-8633.

Savageau, M. A. (1974). Comparison of classical and autogenous systems of regulation in inducible operons. *Nature* **252**, 546-549.

Schedl, A., Ross, A., Lee, M., Engelkamp, D., Rashbass, P., van Heyningen, V. and Hastie, N. D. (1996). Influence of Pax6 gene dosage on development: overexpression causes severe eye abnormalities. *Cell* **86**, 71-82.

Schlake, T., Schropp, M, Maul-Pavicic, A., Malashenko, A. M. and Boehm, T. (2000). Forkhead/winged-helix transcription factor Whn regulates hair keratin gene expression: molecular analysis of the Nude skin phenotype. *Dev. Dyn.* **217**, 368-376.

Scott, G. A. and Goldsmith, L. A. (1993). Homeobox genes and skin development: a review. *J. Invest. Dermatol.* **101**, 3-8.

Stelnicki, E. J, Kömüves, L. G., Kwong, A. O., Holmes, D., Klein, P., Rozenfeld, S., Lawrence, H. J., Adzick, N. S., Harrison, M. and Largman, C. (1998). HOX homeobox genes exhibit spatial and temporal changes in expression during human skin development. *J. Invest. Dermatol.* **110**, 110-115.

Takeuchi, S., Teshigawara, K. and Tkahashi, S. (2000). Widespread expression of Agouti-related protein (AGRP) in the chicken: a possible involvement of AGRP in regulating peripheral melanocortin systems in the chicken. *Biochim. Biophys. Acta* **1496**, 261-269.

Thieffry, D., Huerta, A. M., Perez-Rueda, E. and Collado Vides, J. (1998). From specific gene regulation to genomic networks: a global analysis of transcriptional regulation in Escherichia coli. *BioEssays* **20**, 433-440.

Tkatchenko, A. V., LeCam, G., Léger, J. J. and Dechesne, C. (2000). Large-scale analysis of differential gene expression in the hindlimb muscles and diaphragm of mdx mouse. *Biochim. Biophys. Acta* **1500**, 17-30.

Tomotsune, D., Shoji, H., Wakamatsu, Y., Kondoh, H. and Takanashi, N. (1993). A mouse homologue of the Drosophila tumour-suppressor gene l(2)gl controlled by Hox-C8 in vivo. *Nature* **365**, 69-72.

van der Hoeven, F., Zákány, J. and Duboule, D. (1996). Gene transpositions in the HoxD complex reveal a hierarchy of regulatory controls. *Cell* **85**, 1025-1035.

Wagner-Bernholz, T. J., Wilson, C., Gibson, G., Schuh, R. and Gehring, W. (1991). Identification of target genes of the homeotic gene Antennapedia by enhancer detection. *Genes Dev.* **5**, 2467-2480.

Zeltser, L., Desplan, C. and Heintz, N. (1996). Hoxb-13: a new Hox gene in a distant region of the HOXB cluster maintains colinearity. *Development* **122**, 2475-2484.